

# Closed-Loop Control of The Resonant Flow-Structure Interaction Using PID Controllers

Zhang M. M., Cheng L. & Zhou Y.  
Department of Mechanical Engineering  
The Hong Kong Polytechnic University  
Hung Hom, Kowloon, Hong Kong

## Extended Abstract

The phenomenon of flow-induced vibration due to periodic vortex shedding from a structure, standing in a cross flow, has attracted research interest for many years. Resonant vibration occurs when the natural frequency ( $f_n'$ ) of the structure approaches the frequency of vortex shedding ( $f_s$ ). This type of resonance could have significant impact on the fatigue life of engineering structures, even leading to disastrous consequences.

A novel technique based on structural surface perturbation was recently developed to alter vortex shedding and hence control vortex-induced structural vibration. The local perturbation was made possible by embedding a number of new type of piezo-ceramic curved actuators developed by NASA (THUNDER) on the surface of a bluff body. Experiments were performed in a closed circuit wind tunnel with a square working section (0.6 m  $\times$  0.6 m) of 2.4 m in length. The wind speed of the working section is up to 50 m/s. The free-stream turbulence intensity is less than 0.4%. The test square cylinder of a height  $h = 0.0152$  m, spring-supported at both ends, was allowed to vibrate laterally and spanned the full width of the working section (Fig. 1). Measurements were carried out on the resonance condition of the flow-structure system, i.e.  $f_s \approx f_n'$  ( $= 30$  Hz), of the fluid-cylinder system. The free-stream velocity,  $U_\infty$ , was about 3.58 m/s. The corresponding Reynolds number was about 3500. Three curved piezoelectric actuators (THUNDER) were imbedded in series on the upper side of the cylinder, covered by a plastic plate that was flush with the cylinder surface. When activated, the actuators deformed out of plane to drive this plate oscillating to create the local perturbation on the cylinder surface. The ratio of the perturbation amplitude to the cylinder oscillation amplitude was about 0.35.

In order to further improve the perturbation effect, closed-loop control was introduced in the system using a simple Proportional-integral-derivative (PID) feedback controller. Compared with other control methods, the PID controller has been widely accepted for numerous industrial applications. Its simplicity, robustness and wide range of applicability make it popular in the academic and industry sectors. The development and implementation of the controller was performed using dSPACE system, which greatly simplified the development processes with real-time systems for rapid control prototyping, production code generation, and hardware-in-the-loop tests. A digital signal processor (DSP) with SIMULINK function of MATLAB and software (ControlDesk 2.0) was used for sampling and processing the feedback signal to control the actuators. Proportional gain ( $P$ ), integral gain ( $I$ ) and differential gain ( $D$ ) of PID controller were tuned manually during experiments. The lateral oscillation amplitude, measured by a laser vibrometer, and the streamwise fluctuating velocity from a hot-wire, placed in the upper shear layer ( $x/h = 1.6$ ,  $y/h = -2.5$ ), were used either separately or simultaneously for feedback signals. In order to make sure that a global attenuation is obtained in fluid field, another hot-wire was used as monitoring sensor at  $x/h = 2$ ,  $y/h = 1.5$ , seen in Fig. 1. Using closed-loop control, typical ratio of the perturbation amplitude to the cylinder oscillation amplitude was about 0.07.

Figure 2(a) shows the iso-contour of the normalized spanwise vorticity,  $\omega_z^* = \omega_z h / U_\infty$ , from the PIV measurement when the fluid-structure system is under the resonance condition, i.e.,  $f_s^* = f_n^* = 0.13$  ( $Re = 3500$ ), without any external perturbation. The solid square in the figure indicates the cylinder position. The Kármán vortex street is evident. Using open-loop control, at normalized perturbation frequency  $f_p^* = f_p h / U_\infty = 0.1$ , the Kármán vortex street appeared breaking up (Figure 2(b)) and  $\omega_z^*$  dropped by about 47%. Oppositely, at  $f_p^* = 0.13$ , coincided with

$f_n^*$ , the vortices appeared better organized and larger in size (Figure 2(c)), while  $\omega_z^*$  experienced a jump of 41%. Accordingly, the decrease in circulation ( $\Gamma$ ) exceeded 50% at  $f_p^* = 0.1$  while a conservative estimate of  $\Gamma$  doubled that in Figure 2(a). It was astonishing that at  $f_p^* = 0.13$ , the vortex shedding was subject to impairment instead of enhancement once the PID controllers were switched on, as illustrated by the variation of flow patterns in Figures 2(d)-(f). The shedding action of vortices was almost disappeared (Figure 2(f)) when the feedback signal was from the combination of structural vibration  $Y$  and flow velocity  $u$ . Furthermore,  $\omega_z^*$  and  $\Gamma$  were reduced up to 71% and 65% individually, compared with the unperturbed case (Figure 2(a)), which suggested the significant reduction of vortex strength and more superior control effect than open-loop control even as  $f_p^* = 0.1$  (Figure 2(b)). In addition, by comparing the results from PIV measurements (Figures 2(d)-(f)), it was found that the performance of closed-loop control was improved if the feedback signal from  $u$  was used to replace  $Y$ . The performance was best if a combination of  $Y$  and  $u$  signals was used.

The comparison between open-loop control and closed-loop control was summarized in Table 1. It is easy to note that under closed-loop control, the root-mean-square of both  $Y$  and  $u$  are reduced significantly, up to 82% for  $Y_{rms}$  and 70% for  $u_{rms}$  while the drag coefficient is decreased to 65% of the unperturbed case, which is calculated to the profile of downstream evolution at  $x/h = 3$  from LDA measurement (not shown). In contrast with the most optimum condition of open-loop control ( $f_p^* = 0.1$ ), these results show an improvement though they were achieved with perturbation voltage, 20% that used for open-loop control, indicating the superiority the PID control to the open-loop one.

To investigate the possible physics behind weakening vortex shedding and structural vibration,  $Y$  and  $u$  were measured simultaneously to calculate the shift in phase between them ( $\phi_{Yu} \equiv \tan^{-1}(Q_{Yu} / Co_{Yu})$ ), examined in Figure 3.  $Co_{Yu}$  and  $Q_{Yu}$  are the cospectrum and quadrature spectrum of  $Y$  and  $u$ , respectively. Here, the cross-spectrum is computed from the Fourier transform of the correlation  $\overline{Y(t+\tau)u(t)}$ . Evidently,  $\phi_{Yu}$  (Figure 3(a)) showed a zero phase at  $f_s^* = 0.13$ , indicating the synchronization between  $Y$  and  $u$  signals under no control. The plateau about  $f_s^* = 0.13$  indicated synchronization between the two signals over a range of frequencies about  $f_s^*$ . Once perturbed at  $f_p^* = 0.1$  (Figure 3(b)) by using open-loop control,  $\phi_{Yu}$  was changed from 0 to  $\pi$ , implying the dissipation of  $Y$  and  $u$ . Correspondingly, at  $f_p^* = 0.13$ , the synchronization range in Figure 3(a) was expanded widely (Figure 3(c)), i.e.,  $0.12 < f^* < 0.24$ , indicating the re-enforce of  $Y$  and  $u$ . Though the frequency of the feedback signal or so called perturbation signal ( $f_p^*$ ) still lied at 0.13,  $\phi_{Yu}$  varied from 0 to  $\pi$  instead of remaining 0 as the closed-loop control was exerted, indicating the interaction of  $Y$  and  $u$  was changed from in-phase to anti-phase, shown in Figures 3(d)-(f). In addition, the forced anti-phased effect area on synchronization of  $Y$  and  $u$  in Figure 3(a) expanded extensively, especially when the feedback signal was from the combination of  $Y$  and  $u$  (Figure 3(f)), where  $Y$  and  $u$  collided in the whole coupled range ( $0.11 < f^* < 0.26$ ) followed by open-loop control. These results imply an alteration in the nature of fluid-structure interactions, the in-phased fluid excitation and structural oscillation turning into anti-phased interactions against each other, which dissipates each other in energy and results in drastic weakening vortex shedding and thus structural oscillation. The influence on  $\phi_{Yu}$  was limited within the coupled range ( $0.11 < f^* < 0.26$ ) for the feedback signal from  $Y$  or  $u$  (Figures 3(d)-(e)) and the former was less than the later, which explained the control effect was better when the feedback signal was from  $u$  than  $Y$  (Figures 2(d)-(e)). But low perturbation voltages (Table 1) for the two cases determined the inferiority to open-loop control at  $f_p^* = 0.1$  case.

The investigations up to now lead to the following conclusions:

- 1 PID control has successfully broken the tie of the synchronization range ( $0.11 < f_p^* < 0.26$ ) where the open-loop control fails. Both structural vibration ( $Y$ ) and flow velocity ( $u$ ) can be effectively reduced, up to 82% for  $Y_{max}$  and 70% for  $u_{max}$ , which surpasses the most optimum condition ( $f_p^* = 0.1$ ) of open-loop control.
- 2 With the use of PID control, the required perturbation amplitude or perturbation voltage is greatly reduced, about 1/5 of open-loop control, pointing to the possibility of developing a more compact and self-contained control system.
- 3 Different feedback signals have been used for closed-loop control. It has been found that the control performance is improved if the velocity signal from flow velocity ( $u$ ) is used to replace the structural vibration signal ( $Y$ ). The performance is best if a combination of  $Y$  and  $u$  signals are used. This observation suggests that the key to control flow-induced vibration is to affect the fluid-structure interaction, which in turn reduces vortex shedding, then leading to a structural vibration reduction.

The modeling of fluid-structure interaction is under way especially when a controllable perturbation is introduced, which may hopefully provide us with a better understand of the closed-loop control performance.

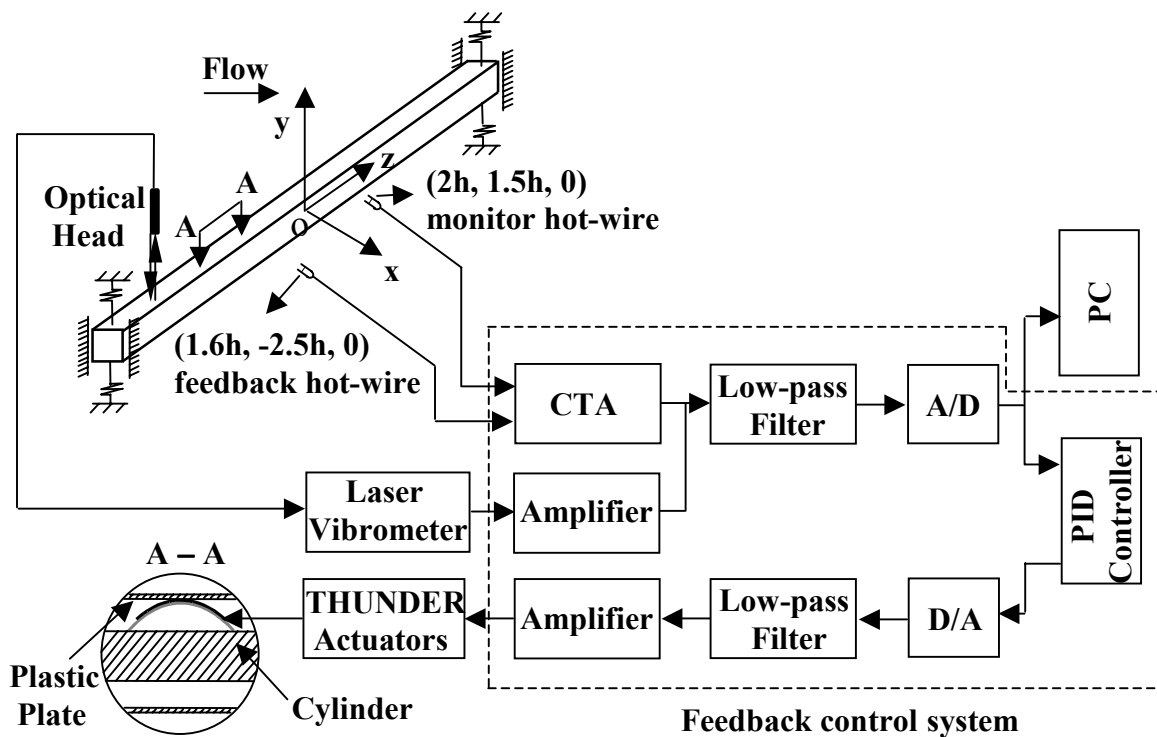


Fig. 1 Experimental Setup.

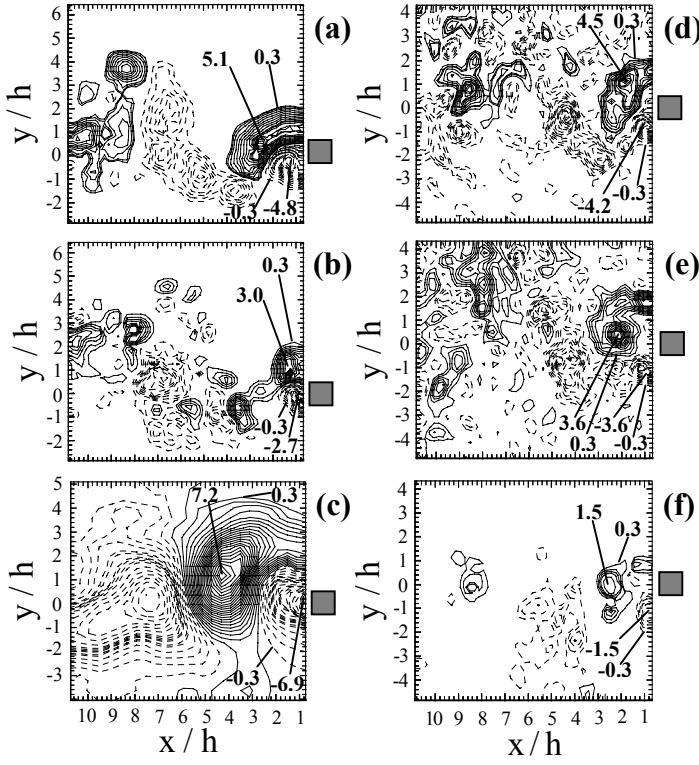


Fig. 2 The iso-contour of spanwise vorticity  $\omega_z^* = \omega_z h / U_\infty$  from PIV measurements with and without control: (a) unperturbed; (b) open-loop control,  $f_p^* = 0.1$ ; (c) open-loop control,  $f_p^* = 0.13$ ; (d) closed-loop control, feedback signal from  $Y$ ,  $P_Y = 1.2$ ,  $I_Y = -0.3$ ,  $D_Y = -0.0004$ ; (e) closed-loop control, feedback signal from  $u$ ,  $P_u = 3.5$ ,  $I_u = 0.2$ ,  $D_u = 0.0001$ ; (f) closed-loop control, feedback signal from the combination of  $Y$  and  $u$ ,  $P_Y = 1.2$ ,  $I_Y = 0.2$ ,  $D_Y = 0.001$ ,  $P_u = 0.4$ ,  $I_u = 0.2$ ,  $D_u = 0.0001$ .

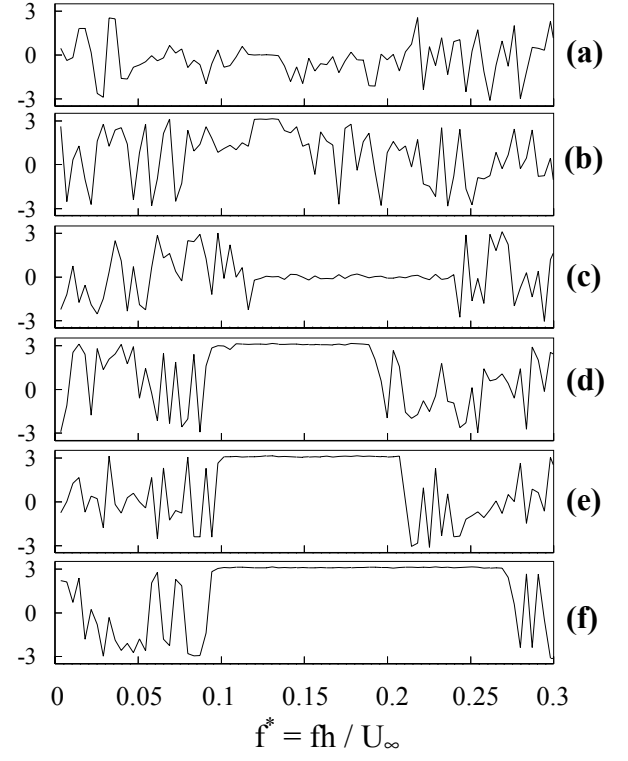


Fig. 3 The phase shift  $\phi_{Y_u}$  between  $Y$  and  $u$  signals with and without control: (a) unperturbed; (b) open-loop control,  $f_p^* = 0.1$ ; (c) open-loop control,  $f_p^* = 0.13$ ; (d) closed-loop control, feedback signal from  $Y$ ,  $P_Y = 1.2$ ,  $I_Y = -0.3$ ,  $D_Y = -0.0004$ ; (e) closed-loop control, feedback signal from  $u$ ,  $P_u = 3.5$ ,  $I_u = 0.2$ ,  $D_u = 0.0001$ ; (f) closed-loop control and feedback signal from the combination of  $Y$  and  $u$ ,  $P_Y = 1.2$ ,  $I_Y = 0.2$ ,  $D_Y = 0.001$ ,  $P_u = 0.4$ ,  $I_u = 0.2$ ,  $D_u = 0.0001$ .

Table 1 The comparison between open-loop control and closed-loop

Control Method	Open-loop $f_p^* = 0.1$		Open-loop $f_p^* = 0.13$		Closed-loop $P_Y = 1.2, I_Y = -0.3, D_Y = -0.0004$		Closed-loop $P_u = 3.5, I_u = 0.2, D_u = 0.0001$		Closed-loop $P_Y = 1.2, I_Y = 0.2, D_Y = 0.001, P_u = 0.4, I_u = 0.2, D_u = 0.0001$	
	$Y_{rms}$	$u_{rms}$	$Y_{rms}$	$u_{rms}$	$Y_{rms}$	$u_{rms}$	$Y_{rms}$	$u_{rms}$	$Y_{rms}$	$u_{rms}$
Fluctuating Percentage	75% ↓	68% ↓	117% ↑	107% ↑	40% ↓	17% ↓	53% ↓	32% ↓	82% ↓	70% ↓
Circulation	50% ↓		97% ↑		22% ↓		34% ↓		65% ↓	
Perturbation Voltage	141.4 volts		141.4 volts		83.7 volts		47.4 volts		27.1 volts	
Drag Coefficient	21% ↓		29% ↑						35% ↓	